Localization of Spiropyran Activation

Martha E. Grady,[1] Cassandra M. Birrenkott,[2] Preston A. May,[§3] Scott R. White,[†4,6] Jeffrey S. Moore,[3,6] Nancy R. Sottos[5,6]*

[1]Department of Mechanical Engineering, University of Kentucky, 506 Administration Drive, Lexington, KY, 40506 USA
[2]Department of Mechanical Engineering, South Dakota School of Mines and Technology, 501 E. Saint Joseph St. Rapid City, SD 57701 USA
[3]Department of Chemistry, University of Illinois at Urbana-Champaign, 505 S. Mathews Avenue, Urbana, IL, 61801, USA
[4]Department of Aerospace Engineering, University of Illinois at Urbana- Champaign, 104 S. Wright Street, Urbana, IL, 61801, USA
[5]Department of Materials Science and Engineering, University of Illinois at Urbana-Champaign, 1304 W. Green Street, Urbana, IL, 61801, USA
[6]Beckman Institute for Advanced Science and Technology, University of Illinois at Urbana-Champaign, 405 N. Mathews Avenue, Urbana, IL, 61801, USA

KEYWORDS: Mechanochemistry, spiropyran, interfacial testing, shear activation, monolayers

ABSTRACT

Functionalization of planar and curved glass surfaces with spiropyran (SP) molecules and localized UV-induced activation of the mechanophore are demonstrated. Fluorescence spectra of UV-irradiated SP-functionalized surfaces reveal that increases in surface roughness or curvature produces more efficient conversion of the mechanophore to the open merocyanine (MC) form. Further, force-induced activation of the mechanophore is achieved at curved glass-polymer interfaces and not planar interfaces. Minimal fluorescence signal from UV-irradiated SP-

functionalized planar glass surfaces precluded mechanical activation testing. Curved glass-polymer interfaces are prepared by SP functionalization of E-glass fibers, which are subsequently embedded in a poly(methyl methacrylate) (PMMA) matrix. Mechanical activation is induced through shear loading by a single fiber microbond testing protocol. *In situ* detection of SP activation at the interface is monitored by fluorescence spectroscopy. The fluorescence increase during interfacial testing suggests that attachment of the interfacial SP molecule to both fiber surface and polymer matrix is present and able to achieve significant activation of SP at the fiber-polymer matrix interface. Unlike previous studies for bulk polymers, SP activation is detected at relatively low levels of applied shear stress. By linking SP at the glass-polymer interface and transferring load directly to that interface, a more efficient mechanism for eliciting SP response is achieved.

INTRODUCTION

The strategy to elicit mechanochemical response from polymeric materials through incorporation of force-sensitive mechanophores has evolved from mechanophore design to ultrasound-induced activation in solution to activation in bulk polymers by deformation.[1-4] Spiropyran (SP) mechanophores have been incorporated into several bulk polymers with varied architectures and the SP to merocyanine (MC) transformation has been studied under diverse loading conditions.[3-7] Several factors that influence SP activation within SP linked polymers include bulk environmental conditions (e.g., temperature),[8-9] polymer architecture,[3, 10-11] polymer chain and mechanophore orientation,[12-13] and polymer time-dependence.[14] Attachment of polymer chains to a mechanophore is critical for transduction of mechanical force in bulk polymers, though recent work on SP pulling point location demonstrated that SP-linked bulk polymers are less sensitive than predicted to pulling point location.[15] Likewise, we observed that covalent attachment

to the mechanophore is also critical for transduction of mechanical force across an interface of dissimilar materials.

Beyond self-reporting bulk polymers, investigators have sought to harness the tension-sensing capabilities of mechanophores at interfaces. Applications for these types of interfacial mechanophore systems include monitoring bimolecular reactions[16] composite interfaces,[17] and living-nonliving interfaces in biology.[18] To realize SP as one such self-reporting molecular tether, basic factors that influence *in situ* reactivity (e.g., temperature, light, pH) and substrate choice have been reported. SP-functionalized fused silica was the platform chosen to probe photocoloration, photobleaching and thermal fading reactions of SP through the use of Brewster angle microscopy.[19] The thermo- and photo-transformations of SP absorbed on a silver film were studied by Raman scattering spectroscopy.[20] Doron *et al*.[21] functionalized gold electrodes with an assembled monolayer of SP, demonstrating the capability of the photo-, thermo-, and pH- stimulated interface to control electrooxidation. Rosario *et al*.[22] demonstrated that separation of neighboring SP molecules on a planar surface resulted in increased UV-activated water contact angle change. The separation was achieved by tertbutyldiphenylsilyl groups blocking surface attachment of SP molecules and was hypothesized to lead to a less restrictive geometry so that the photochromic reaction could take place with minimal steric hindrance. As a follow up, they showed that increased surface roughness by silicon nanowires amplified the photochromic response.[23] After this initial work, wettability switching of spiropyrans was studied by several groups[24-25] and led to new light-responsive drug carriers.[26] These advances capitalize on photo-initiated SP to MC conversion, yet mechanical activation is required for mechanophores to form tension-sensing interfaces. Mechanical activation of mechanophores sequestered at an interface is challenging. Recently, new methodology was developed to characterize mechanical activation of maleimide–anthracene

mechanophores at a solid interface.[27] Sung *et al*., loaded the mechanophore-functionalized interface by laser-induced stress waves and reported covalent attachment was required for activation. We have incorporated a covalent attachment strategy for SP and report on the mechanical activation of SP mechanophores across a polymer-glass interface at low levels of applied shear stress.

In this work, a single fiber microbond test protocol[28-30] is adopted to impart force to SP-functionalized fibers embedded in a polymer matrix. A tensile force is applied to the fiber, subjecting the mechanophore-functionalized interface to highly localized shear forces. The interfacial shear stress developed along the embedded length of the fiber reaches a maximum near the edge of the fiber. Photo-initiated activation is shown for the SP-functionalized fibers and compared to SP-functionalized planar substrates of silicon and fused silica. The reactivity of SP functionalized planar substrates are compared to the reactivity of functionalized fibers.

EXPERIMENTAL SECTION

Interfacial SP Synthesis. An interfacial SP molecule (**1**) capable of covalent bonding across a glass fiber-poly(methyl methacrylate) (PMMA) polymer matrix interface was synthesized with a carboxylic acid functionality at the 5' position and a methacrylate functionality at the 8 position (Scheme 1a). A monofunctional SP molecule (**2**) was also created (Scheme 1b) with functionality to covalently bond to the fiber surface but contained no functionality to covalently bond to the polymer matrix.

a) Interfacial SP **(1)** b) Monofunctional SP **(2)**

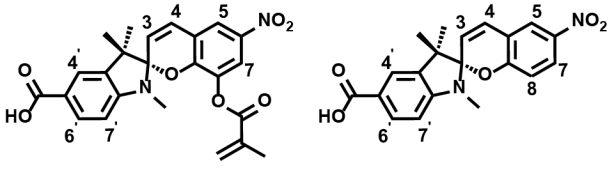

Scheme 1. Interfacial SP molecules. a) Interfacial SP **(1)** with carboxylic acid at the 5' position for fiber attachment and a methacrylate at the 8 position for PMMA attachment. b) Monofunctional SP **(2)** contains carboxylic acid at the 5' position for fiber attachment, but no functionality for polymer attachment.

Interfacial SP-functionalized Planar Surfaces. SP monolayer functionalization was accomplished in a molecular layer-by-layer process. First, glass substrates were functionalized with 3-aminopropyltriethoxysilane (APS), followed by active or monofunctional SP (Scheme 1). The self-assembly process yields a surface where the amine-terminated SAMs serve as a platform for SP attachment. Glass and silicon substrates were cleaned in piranha solution (3 H_2SO_4 : 1 H_2O_2 by volume) at 120 °C for 60 min to remove any organic material from the substrate surface. The substrates were then rinsed with deionized water, dried under a stream of air, and further dried in an oven at 140 °C for at least 5 min. Substrates were immersed into a 10 mM solution of APS in 20 mL of toluene for 30 min then rinsed with toluene followed by deionized water and dried at 140 °C for 30 min. The SAM-modified substrates were then immersed in a 1 mM solution of SP ((**1**) or (**2**)) in 10 mL of ethanol and 0.2 g of carbodiimide (1-ethyl-3-(3-dimethyleaminopropyl)carbodiimide (EDC)).

Confirmation of SP-functionalized Planar Surfaces. Atomic force microscopy (AFM) and ellipsometry were used to obtain surface height information and molecular layer thickness respectively. Monolayer thickness was characterized using a single-wavelength (633 nm) ellipsometer (Gaertner L116C). Because of the similarity in the refractive index of SiO2 and alkyl SAMs, ellipsometry could not be conducted directly on glass substrates. Thus, for ellipsometric measurements, SAMs were concurrently deposited on silicon substrates in the same reaction

vessel. A refractive index of 1.5 was used for the molecular layers, and substrate parameters were used from ellipsometric measurements of bare silicon from the same wafer. Ellipsometric measurements were taken at three locations on the functionalized surface, where three measurements were repeated in each location to ensure uniformity. Measurements were taken after functionalization with APS and after SP functionalization. An estimate of the SP monolayer thickness (7 Å) was made from subtracting the APS layer thickness from the total thickness measurement after SP functionalization. Ellipsometric measurements for molecular functionalization are summarized in Figure 1. Functionalization with APS resulted in a molecular layer on the order of 5 Å. After SP functionalization, the total layer thickness was 11-12 Å.

AFM was conducted in tapping mode using a Cypher AFM system (Asylum Research) to provide surface height information, from which a surface roughness, the root mean square from average (RMS), was calculated. AFM scans on at least three different locations were performed on functionalized surfaces with a typical window of 1 x 1 μm at a scan rate less than 3 Hz. The average surface roughness for each functionalization on silicon substrates are reported in Figure 1. On average, silicon surfaces with active SP (1) and monofunctional SP (2) each had an RMS of 1.8 Å. SP functionalization did not drastically alter the surface roughness of SAM only functionalization.

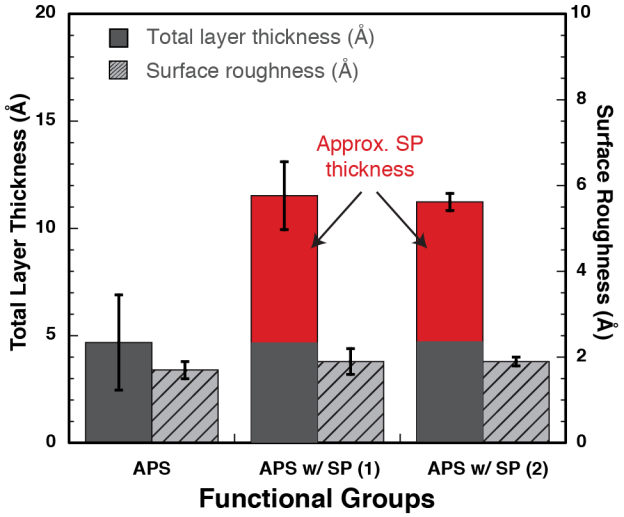

Figure 1. Ellipsometry measurements of layer thickness (solid bars) and AFM surface roughness (patterned bars) of silicon substrates functionalized with APS only, APS with SP (**1**), and APS with SP (**2**). Red shading represents SP thickness of approximately 7 Å.

Interfacial SP-functionalized Fibers. Following a similar procedure to that for functionalization of glass and silicon substrates, E-glass fibers, 16 μm in diameter (Owens Corning 158B-AA-675) with a proprietary aminopropylsilane (APS) sizing were functionalized with interfacial SP. SP ((**1**) or (**2**)) was dissolved in tetrahydrofuran (THF) with an activating agent, EDC, and the E-glass fibers were stirred in the solution for 72 hours, allowing sufficient time for the carboxylic acid and APS to form an amide bond, covalently attaching the SP to the fiber surface. Fibers were removed from the solution, rinsed with water and THF, soaked in THF for 4 hours, and rinsed again with THF and water to wash away SP not covalently bound to the fiber surface. Fibers were dried in a 35°C oven for 12 hours to remove remaining solvent.

Polymer Matrix Synthesis. Synthesis of linear PMMA matrix was performed via a free radical polymerization using benzoyl peroxide (BPO) as the radical source and N,N-dimethylaniline

(DMA) as the activator as described by Kingsbury *et al*.[7] Methyl methacrylate (MMA) (1 mL, 9.39 mmol, 1 equiv.) and BPO (15 mg, 0.0619 mmol, 0.00662 equiv.) were combined in a scintillation vial, flushed with argon, and sealed with a septum. Ethyl phenylacetate (EPA) (0.4 mL, 2.51 mmol, 0.267 equiv.) was added to the solution to lengthen the working time during polymerization. Once the BPO was fully dissolved, DMA (6 μL, 0.0473 mmol, 0.00506 equiv.) was injected into the scintillation vial.

Preparation of Single Fiber Microbond Specimens. Microbond specimens were fabricated following the method of Blaiszik *et al*.[28] and a side-view schematic is shown in Figure 2. A SP-functionalized glass fiber was placed on top of parallel non-functionalized support fibers resting on an acrylic substrate. The MMA solution was allowed to pre-polymerize for 3 hours to increase viscosity. A small drop of solution was then deposited on the functionalized fiber in an argon environment (Vacuum Atmospheres Company MO-20 glove box). A small glass cover slip (≅5x5x1 mm) was placed on the monomer droplet to create a flat specimen surface. Specimens were allowed to polymerize for 8 hours in the argon environment and were then held at 40°C under vacuum for 8 hours to remove remaining EPA. Paper tabs were adhered to the functionalized fiber to facilitate gripping during interfacial loading.

Several types of specimens were produced by varying the possible attachment points of the interfacial SP molecule and are summarized in Table 1. Type 1 specimens were prepared with the interfacial SP molecule (**1**) and a PMMA polymer matrix. By applying the MMA solution before full polymerization, the methacrylate functional group at the 8 position of the interfacial SP molecule (**1**) is forced to covalently bond to the polymer at the fiber-polymer interface. Type 2 specimens were created with the interfacial SP molecule (**1**) and an epoxy matrix, allowing for covalent bonding of SP to the fiber surface, but eliminating covalent linking to the polymer matrix.

Type 3 specimens were produced with glass fibers functionalized according to the procedure described above but lacked the activating agent EDC during functionalization. In this case, the interfacial SP molecule (**1**) was attached to the fiber surface by only electrostatic forces. The SP molecules remaining on the surface by electrostatic forces after the rinsing procedure can, however, covalently attach to the PMMA matrix. Type 4 specimens were prepared with plain, unsized glass fibers and PMMA matrix, and contained no SP. Glass fibers functionalized with monofunctional SP (**2**) were used for Type 5 specimens. The monofunctional SP molecule (**2**) is capable of covalently attaching to the fiber surface, but without the methacrylate functionality at the 8 position, cannot covalently attach to the PMMA matrix.

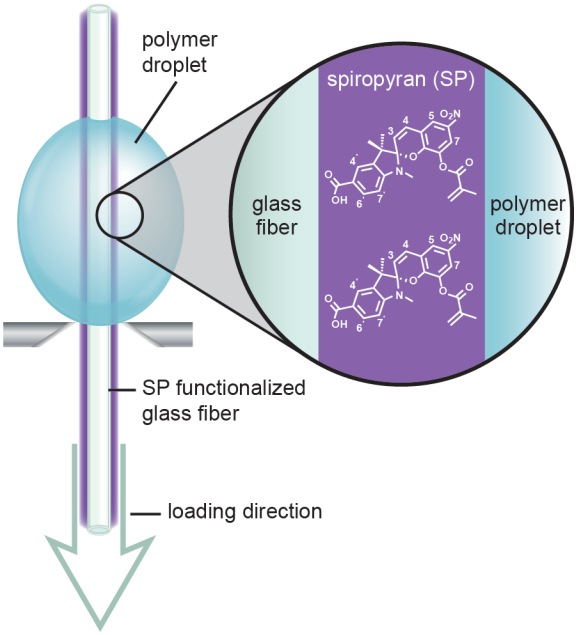

Figure 2. Side-view schematic of an active single fiber microbond specimen.

Table 1. Specimen type and corresponding SP molecule with available covalent attachment sites.

Specimen Type	Fiber functionalization	Polymer matrix	SP molecule attachment
Type 1	Interfacial SP (**1**)	PMMA	fiber & polymer matrix
Type 2	Interfacial SP (**1**)	epoxy	fiber
Type 3	Interfacial SP (**1**)	PMMA	polymer matrix
Type 4	None	PMMA	n/a
Type 5	Monofunctional SP (**2**)	PMMA	fiber

Interfacial Shear Testing and *in situ* Fluorescence Spectroscopy. The functionalized fiber was loaded in tension at 0.5 μm/sec with a Physik Instrument M-230.10S linear actuator until interfacial debond was achieved. Load was monitored using a Honeywell Sensotec (150 g) load cell. Load and displacement were collected and correlated using a LabVIEW program. During interfacial testing, the load increased until complete interfacial debond, at which point the load dropped quickly before plateauing to a frictional load value. Crosshead displacement was determined directly from the linear actuator. The average interfacial shear stress, τ_{int}, was calculated as

$$\tau_{int} = \frac{P}{\pi \cdot d \cdot l_e}, \qquad (1)$$

where P is the measured load, d is the fiber diameter, and l_e is the embedded length of fiber in the polymer matrix as measured optically before testing.[28-29, 31-32] During loading, the local shear stress near the edge of the specimen is significantly higher, leading to localized plastic deformation of the PMMA matrix in close proximity to the interface.

In situ fluorescence spectra were collected during interfacial loading using a Horiba LabRAM HR Raman spectroscopy imaging system. An excitation beam of 532 nm was incident upon the specimen, focused on the surface of the fiber embedded in the polymer matrix. Wavelengths of

550-750 nm were collected at regular intervals during interfacial loading and a shutter was used to block the excitation laser between spectra collection to minimize the effects of photobleaching.

The fluorescence emission peak of the mechanically activated MC is broad and centered near 625 nm. As such, the activation intensity (I_{act}) was defined as

$$I_{act} = \frac{I(620-630nm)}{I(620-630nm)_{t=0}}, \qquad (2)$$

where I(620-630nm) is the average intensity between 620-630 nm and I(620-330 nm)t=0 is the average intensity between 620-630 nm of the initial spectra taken after bleaching and before deformation.

RESULTS AND DISCUSSION

UV-induced Activation of SP-functionalized Planar Surfaces. Fluorescence spectroscopy was used to characterize photo-activation of SP-functionalized glass and silicon surfaces. Fluorescence spectra were recorded after UV irradiation on bare substrates, substrate/SAMs and substrate/SAM/SP specimens, and the closing of the substrate/SAM/SP specimens with a 532 nm laser. Specimens were irradiated with a UV lamp (Black-Ray Longwave Ultraviolet Lamp Model B 100AP) for 10 min at an intensity > 2 mW/cm^2. The intensity of the UV lamp was measured using a digital UV meter (General Tool UV513AB Digital UVAB Meter for Ultraviolet Light Measurement). Activation of SP molecules is indicated by a peak in the fluorescence signal emerging around 600 nm.

The fluorescence signals from functionalized substrates are included in Figure 3. Activation of SP-functionalized planar glass substrates (Figure 3 a,b) resulted in higher fluorescence peaks than SP-functionalized planar silicon substrates (Figure 3 c,d). Signals from UV-activated

monofunctional interfacial SP (**2**) (Figure 3 b,d) resulted in higher fluorescence peaks than UV-activated active interfacial SP (**1**) (Figure 3 a,c). One possible explanation for the difference in fluorescence activity between two planar substrates with the same surface chemistry (SiO_2) could be due to the large difference in surface roughness. Silicon is almost 10 times smoother than polished fused silica, even after self-assembled monolayer deposition.[33] The larger surface roughness could allow two outcomes 1) more SP could assemble on the rough surface in the same linear length resulting in higher fluorescence or 2) larger roughness increases the distance between nearest neighboring SP molecules therefore decreasing steric hindrance, which could be a large factor in UV activation of SP on planar glass slides. Rosario *et al*.[22] found an increase in UV activation of SP when a blocker, TBDS, was used in addition to APS to "dilute the surface coverage of the bound SPCOOH so as to meet the steric demands of the spiropyran." Thus, we believe the reduction in steric hindrance due to higher surface roughness increased the fluorescence activity of the planar glass substrates compared to the planar silicon substrates.

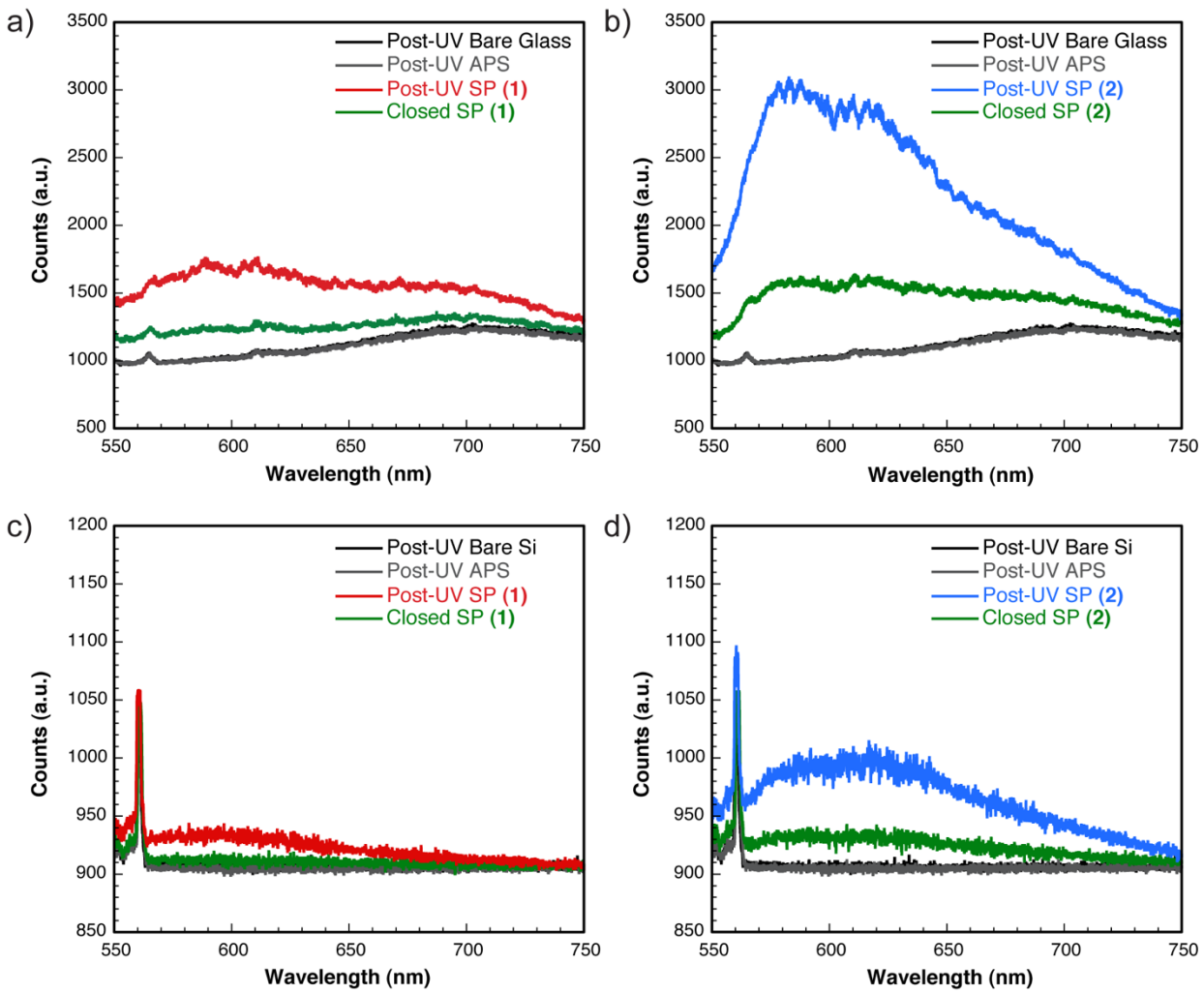

Figure 3. Fluorescence spectra after UV-irradiation for functionalized substrates. a) Bare glass, APS-functionalized glass, and SP (**1**) on APS-functionalized glass, b) bare glass, APS-functionalized glass, and SP (**2**) on APS-functionalized glass, c) bare Si, APS-functionalized Si, and SP (**1**) on APS-functionalized Si, and d) bare Si, APS-functionalized Si, and SP (**2**) on APS-functionalized Si. The fluorescence spectra of SP functionalized substrates after irradiation with 532 nm wavelength light (closes the SP) is shown in green. Bare substrates are shown in black, substrates with APS only are shown in gray, SP (**1**) functionalized surfaces are shown in red, and SP (**2**) functionalized surfaces are shown in blue.

UV-induced Activation of SP-functionalized Fibers. Fiber functionalization was confirmed through fluorescence spectra of fibers with varied functionalization prior to polymer matrix application. Fibers were placed in dark conditions for a minimum of 15 minutes to allow SP to reach a photostationary equilibrium with the MC form[22] prior to collecting fluorescence spectra. Spectra were collected (Figure 4) from fibers used to prepare each specimen type in Table 1. Fibers with a covalently bound interfacial SP molecule **(1)** (Type 1 and Type 2) emit a broad fluorescence peak centered near 600 nm, consistent with fluorescence spectra of SP molecules bound to glass substrates collected by Rosario *et al*.[22] Fibers used for Type 3 specimens with the interfacial SP molecule **(1)** only able to attach to the surface by electrostatic forces exhibit a lower intensity than Type 1 and Type 2 fibers, indicating that more interfacial SP **(1)** adheres to the fiber surface when covalently bonded. Fibers containing no SP (Type 4) have very little fluorescence signal, as expected. Fibers with covalently bound monofunctional SP **(2)** used for Type 5 specimens show a very strong fluorescence signal which is characteristically different than that of Type 1 or Type 2 fibers, showing double peaks centered near 580 nm and 625 nm. The magnitude in fluorescence intensity outstrips that of the planar substrates by an order of magnitude. A glass fiber naturally has an increase in roughness (defined as a deviation from planar in this case) and so contributes to the surface roughness theory developed earlier to explain the difference in fluorescence activation between planar glass and planar silicon. Nygård *et al*.,[34] used a 3rd order surface fit to remove the saddle-like curvature of a glass fiber to obtain the surface roughness and found an average roughness of 12 Å. The value of surface roughness including the curvature could be an order of magnitude larger, thus emphasizing the difference in our SP grafted surfaces: planar silicon (1.8 Å), planar glass (7.4 Å)[33], and glass fiber (> 12 Å)[34], in order of increasing surface roughness, which also corresponds to an increasing fluorescence intensity from UV-activation.

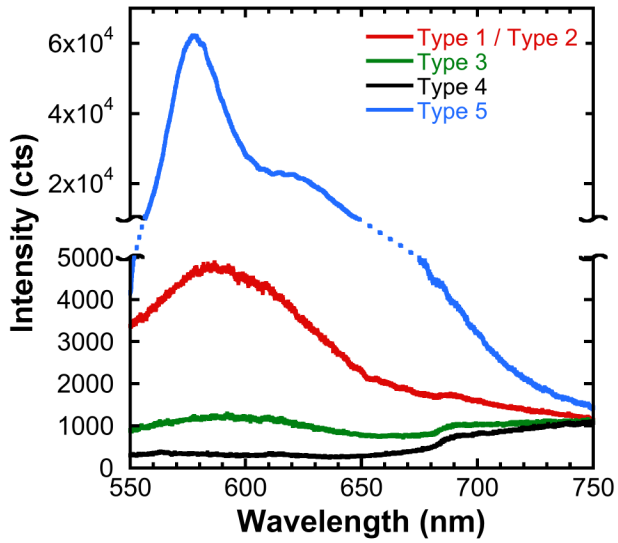

Figure 4. Fluorescence spectra of functionalized fibers used to make each specimen type.

Mechanical Activation of Interfacial SP. Each specimen type in Table 1 was tested while simultaneously collecting load, displacement, and fluorescence intensity. Interfacial shear stress is correlated with activation intensity, I_{act}, as calculated from Equation 2, and representative behavior of each specimen type is shown in Figure 5. For each specimen type, the average interfacial shear stress increases linearly until dropping suddenly at full interfacial debonding. Type 1 (Figure 5a) exhibits a large increase of activation intensity at the peak stress level, just before full interfacial debonding. Type 2 specimens, where the interfacial SP molecule (1) is only covalently bound to the fiber surface, show a very small increase in activation intensity due to interfacial testing (Figure 5b). Figure 5c contains representative behavior of Type 3, with interfacial SP (1) covalently bound to only the polymer matrix. Again, only a slight increase in activation intensity is measured during interfacial debonding. Type 4, containing no SP, also produced a small amount of fluorescence intensity during interfacial testing (Figure 5d). We hypothesize that this small increase is associated with refraction due to interfacial damage during the debonding process. Finally, Type 5, containing monofunctional SP (2), exhibits significantly larger activation intensity during

interfacial debonding (Figure 5e) than Type 1-4. The large increase of activation intensity during interfacial debonding of specimen Type 1 and Type 5 indicates successful transformation of SP to the open, fluorescent MC form.

The average activation intensity after full interfacial debond is compared for each specimen type in Figure 6. The fluorescence increase during interfacial testing of Type 1 is statistically higher than Type 2, Type 3 or Type 4, suggesting that covalent attachment of the interfacial SP molecule (1) to both the fiber surface and the polymer matrix is required to achieve significant activation of SP at the fiber-polymer matrix interface. Although local shear stress may reach high levels, the applied average shear stress to induce mechanochemical reactivity of an interfacial SP molecule (1) is significantly lower than was required for activation of bulk SP-crosslinked PMMA in torsion.[7]

In addition to collecting fluorescence spectra during interfacial debonding, a fluorescence polarization technique developed by Beiermann *et al*.[13] for measurement of SP mechanophore alignment was adapted to the Raman spectrometer by placing a polarizer and analyzer in the path of the excitation and emission beam, respectively. As described by Beiermann, an order parameter, S, designates the degree of SP orientation and is calculated as

$$S = \frac{\left(I_{\parallel} - I_{\perp}\right)}{\left(I_{\parallel} + 2I_{\perp}\right)}, \qquad (3)$$

where $I_{\parallel}$ and $I_{\perp}$ are the total fluorescence intensity collected with the analyzer parallel and perpendicular to the loading direction, respectively. The order parameter varies between 0 (random SP orientation) and 1 (perfect SP orientation).

Orientation of the interfacial SP was measured before and after interfacial testing for a Type 1 specimen containing the interfacial SP molecule (**1**) and for a Type 5 specimen containing the monofunctional SP molecule (**2**). Table 2 shows the change in order parameter due to interfacial debonding. In a Type 1 specimen, the interfacial SP molecule (**1**) exhibited a large increase in SP orientation with the direction of loading after interfacial debonding. Alignment and mechanochemical activation of the interfacial SP molecule (**1**) during interfacial testing of Type 1 specimens was consistent with previous studies suggesting mechanophore orientation promotes activation.[13] The monofunctional SP molecule (**2**) in a Type 5 specimen showed virtually no change in SP orientation with the direction of loading after interfacial debonding.

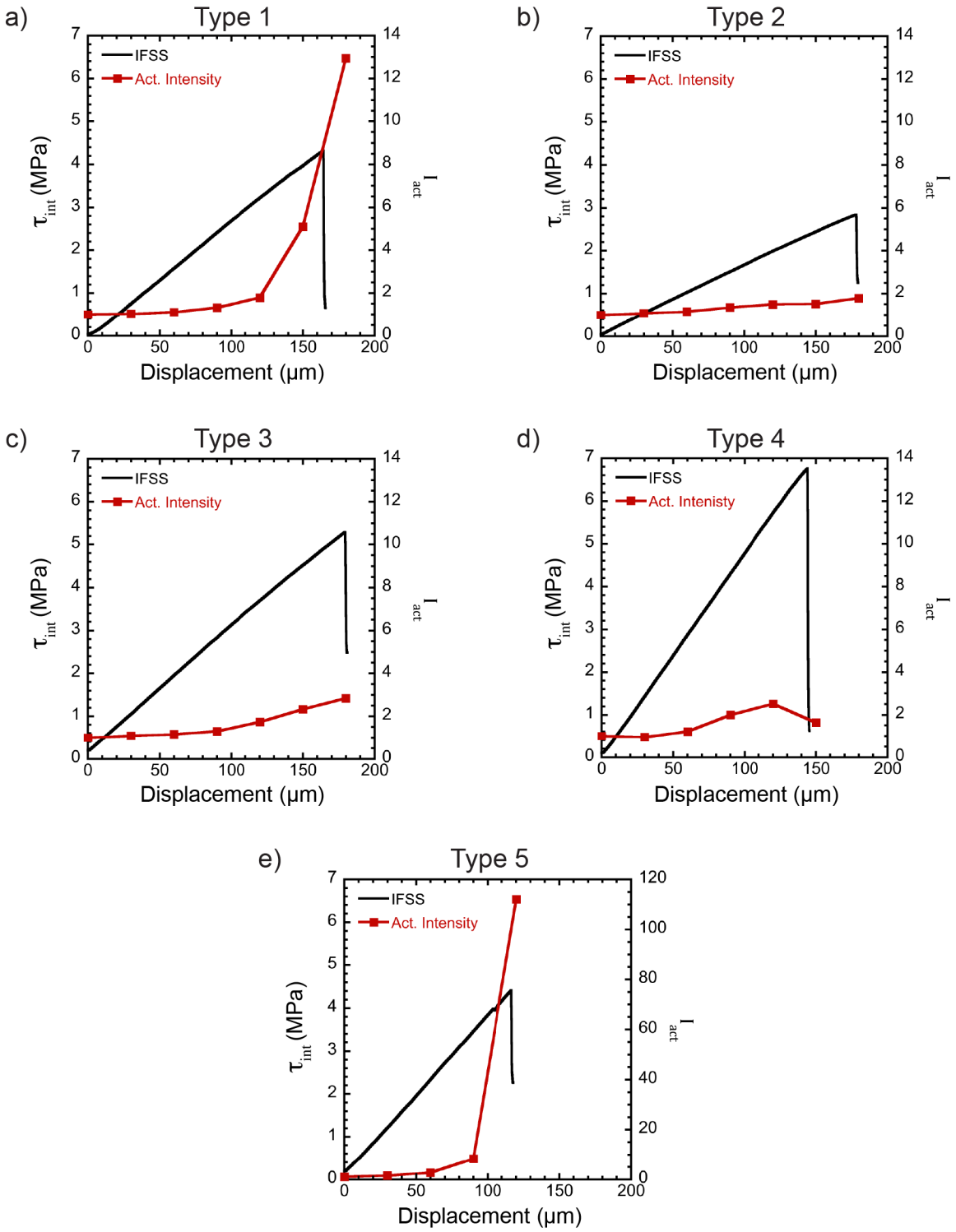

Figure 5. Representative interfacial shear stress (τ_{int}) and activation intensity (I_{act}) as a function of displacement for each specimen type.

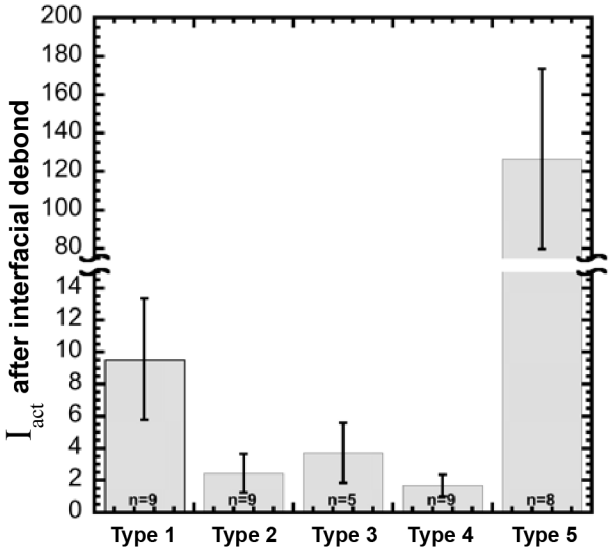

Figure 6. Average activation intensity after interfacial debonding for each specimen type. Error bars reflect one standard deviation.

Table 2. Change in order parameter for specimen Type 1 and Type 5 due to interfacial testing.

Specimen Type	Interfacial SP molecule	Change in Order Parameter, *S* due to interfacial debonding
Type 1	Interfacial SP (**1**)	0.195
Type 5	Monofunctional SP (**2**)	-0.002

CONCLUSIONS

The functionalization of planar silicon and glass substrates with single monolayers of two species of SP mechanophores was accomplished by successive self-assembly processes. Substrates were first functionalized with an amine-terminated SAM and then with two different forms of interfacial SP. The increase in specimen thickness at each step was confirmed by ellipsometry. Furthermore, the relatively smooth functionalized surfaces confirmed by AFM provide evidence that a single monolayer was formed. Activation of SP monolayers was demonstrated by UV-induced fluorescence and increased in intensity with increasing surface roughness. We believe the

reduction in steric hindrance afforded by an increase in surface roughness, thereby increasing the distance between neighboring spiropyrans, ultimately led to an increase in UV activation of both SP forms. This result is in line with previous work by Rosario *et al*.[23] who showed amplification of stimulus-induced contact angle switching due to increased surface roughness. Increased surface roughness overcomes steric constraints found during photoisomerization of adsorbed monolayers of other photochromic molecules on planar surfaces.[35]

In addition to SP monolayer characterization on planar substrates, a SP mechanophore was successfully attached to the surface of a commercial E-glass fiber. Confirmation of the presence of SP on the fiber surface was provided by UV-induced fluorescence spectra, which exhibited a remarkable increase in fluorescence intensity compared to the planar substrates. Single fiber microbond specimens were prepared with fibers of varied functionality and different polymer matrices, allowing for control of the SP covalent attachment sites. Load was applied to the functionalized fiber to induce interfacial debonding and the calculated interfacial shear stress was correlated to *in situ* fluorescence spectra. The mechanical activation of the interfacial SP molecule was observed as an increasing fluorescence peak centered near 625 nm. Higher activation intensity was measured for specimens with SP linked covalently to both the fiber surface and polymer matrix than for specimens with SP linked to either the fiber or the polymer matrix, implying the need for covalent linking across the SP molecule to achieve appreciable mechanochemical activation. Contrasting previous studies for bulk polymers, which achieved SP activation at shear stress levels at or above 20 MPa,[7,14] SP activation was detected at low levels of applied shear stress (< 5 MPa). We show that covalent linking of SP at the glass-polymer interface transferred the load directly to the interface, resulting in a change in the orientation of the SP molecule and a more efficient mechanism for eliciting SP response.

ASSOCIATED CONTENT

Supporting Information. Chemical structures and details of synthesis. This material is available free of charge via the Internet at http://pubs.acs.org.

AUTHOR INFORMATION

Author E-mail Addresses: cassandra.birrenkott@sdsmt.edu (Cassandra M. Birrenkott), m.grady@uky.edu (Martha E. Grady), preston.may@halliburton.com (Preston A. May), jsmoore@illinois.edu (Jeffrey S. Moore), n-sottos@illinois.edu (Nancy R. Sottos)

†Scott R. White made significant intellectual contributions prior to his passing on May 28th, 2018, and is therefore included as a co-author.

Present Address

§Dr. Preston May
Halliburton Energy Services
3000 N Sam Houston Pkwy E
Houston, TX 77032

Corresponding Author

*Assistant Professor Martha E. Grady
Department of Mechanical Engineering
University of Kentucky
506 Administration Drive
Lexington, KY 40506
E-mail: m.grady@uky.edu
ORCID: 0000-0002-1767-3653

Author Contributions

The manuscript was written through equal contributions of M.E.G., C.M.B., P.A.M., J.S.M, and N.R.S. These authors have given approval to the final version of the manuscript.

Funding Sources

Funding was provided by the ARO MURI W911NF-07-0409 and the National Science Foundation, CMMI 11-61517.

ACKNOWLEDGMENT

The authors gratefully acknowledge the Beckman Institute for Advanced Science and Technology for their assistance in this work. Experiments were carried out in part in the Frederick Seitz Materials Research Laboratory Central Research Facilities and the Beckman Institute Imaging

Technology Group, University of Illinois. The authors also thank Nicholas Munaretto for assistance with SP synthesis and Amanda Jones for helpful insight into single fiber testing.

ABBREVIATIONS

SP, spiropyran; MC, merocyanine; PMMA, poly(methyl methacrylate); UV, ultraviolet light; APS, 3-aminopropyltriethoxysilane; EDC, 1-ethyl-3-(3- dimethyleaminopropyl)carbodiimide; AFM, atomic force microscopy; RMS, root mean square; THF, tetrahydrofuran; BPO, benzoyl peroxide; DMA, N,N-dimethylaniline; MMA, methyl methacrylate; EPA, ethyl phenylacetate;

REFERENCES

1. Li, J.; Nagamani, C.; Moore, J. S., Polymer Mechanochemistry: From Destructive to Productive. *Acc. Chem. Res.* **2015,** *48* (8), 2181-2190.

2. Black, A. L.; Lenhardt, J. M.; Craig, S. L., From molecular mechanochemistry to stress-responsive materials. *J. Mater. Chem.* **2011,** *21* (6), 1655-1663.

3. Davis, D. A.; Hamilton, A.; Yang, J. L.; Cremar, L. D.; Van Gough, D.; Potisek, S. L.; Ong, M. T.; Braun, P. V.; Martinez, T. J.; White, S. R.; Moore, J. S.; Sottos, N. R., Force-induced activation of covalent bonds in mechanoresponsive polymeric materials. *Nature* **2009,** *459* (7243), 68-72.

4. Klajn, R., Spiropyran-based dynamic materials. *Chem. Soc. Rev.* **2014,** *43* (1), 148-184.

5. Beiermann, B. A.; Davis, D. A.; Kramer, S. L. B.; Moore, J. S.; Sottos, N. R.; White, S. R., Environmental effects on mechanochemical activation of spiropyran in linear PMMA. *Journal of Materials Chemistry* **2011,** *21* (23), 8443.

6. Grady, M. E.; Beiermann, B. A.; Moore, J. S.; Sottos, N. R., Shockwave Loading of Mechanochemically Active Polymer Coatings. *Acs Appl. Mater. Inter.* **2014,** *6* (8), 5350-5355.

7. Kingsbury, C. M.; May, P. A.; Davis, D. A.; White, S. R.; Moore, J. S.; Sottos, N. R., Shear activation of mechanophore-crosslinked polymers. *J. Mater. Chem.* **2011,** *21* (23), 8381-8388.

8. Kim, J. W.; Jung, Y.; Coates, G. W.; Silberstein, M. N., Mechanoactivation of Spiropyran Covalently Linked PMMA: Effect of Temperature, Strain Rate, and Deformation Mode. *Macromolecules* **2015,** *48* (5), 1335-1342.

9. Beiermann, B. A.; Davis, D. A.; Kramer, S. L. B.; Moore, J. S.; Sottos, N. R.; White, S. R., Environmental effects on mechanochemical activation of spiropyran in linear PMMA. *J. Mater. Chem.* **2011,** *21* (23), 8443-8447.

10. Lee, C. K.; Beiermann, B. A.; Silberstein, M. N.; Wang, J.; Moore, J. S.; Sottos, N. R.; Braun, P. V., Exploiting Force Sensitive Spiropyrans as Molecular Level Probes. *Macromolecules* **2013,** *46* (10), 3746-3752.

11. O'bryan, G.; Wong, B. M.; McElhanon, J. R., Stress Sensing in Polycaprolactone Films via an Embedded Photochromic Compound. *Acs Appl. Mater. Inter.* **2010,** *2* (6), 1594-1600.

12. Lee, C. K.; Davis, D. A.; White, S. R.; Moore, J. S.; Sottos, N. R.; Braun, P. V., Force-Induced Redistribution of a Chemical Equilibrium. *J. Am. Chem. Soc.* **2010,** *132* (45), 16107-16111.

13. Beiermann, B. A.; Kramer, S. L. B.; Moore, J. S.; White, S. R.; Sottos, N. R., Role of Mechanophore Orientation in Mechanochemical Reactions. *Acs Macro Lett* **2012,** *1* (1), 163-166.

14. Degen, C. M.; May, P. A.; Moore, J. S.; White, S. R.; Sottos, N. R., Time-Dependent Mechanochemical Response of SP-Cross-Linked PMMA. *Macromolecules* **2013,** *46* (22), 8917-8921.

15. Kim, T. A.; Robb, M. J.; Moore, J. S.; White, S. R.; Sottos, N. R., Mechanical Reactivity of Two Different Spiropyran Mechanophores in Polydimethylsiloxane. *Macromolecules* **2018,** *51* (22), 9177-9183.

16. Kersey, F. R.; Yount, W. C.; Craig, S. L., Single-Molecule Force Spectroscopy of Bimolecular Reactions: System Homology in the Mechanical Activation of Ligand Substitution Reactions. *J. Am. Chem. Soc.* **2006,** *128* (12), 3886-3887.

17. Manivannan, M. S.; Silberstein, M. N., Theoretical framework and design of mechanochemically augmented polymer composites. *Extreme Mechanics Letters* **2018,** *19*, 27-38.

18. Liu, Y.; Yehl, K.; Narui, Y.; Salaita, K., Tension Sensing Nanoparticles for Mechano-Imaging at the Living/Nonliving Interface. *J. Am. Chem. Soc.* **2013,** *135* (14), 5320-5323.

19. Gorelik, S.; Hongyan, S.; Lear, M. J.; Hobley, J., Transient Brewster angle reflectometry of spiropyran monolayers. *Photoch Photobio Sci* **2010,** *9* (2), 141-151.

20. Vasilyuk, G. T.; Maskevich, S. A.; Podtynchenko, S. G.; Stepuro, V. I.; Lukyanov, B. S.; Alexeenko, Y. S., Structural thermo- and phototransformations of oxaindane spiropyrans adsorbed on silver films. *Journal of Applied Spectroscopy* **2002,** *69* (3), 344-350.

21. Doron, A.; Katz, E.; Tao, G. L.; Willner, I., Photochemically-, chemically-, and pH-controlled electrochemistry at functionalized spiropyran monolayer electrodes. *Langmuir* **1997,** *13* (6), 1783-1790.

22. Rosario, R.; Gust, D.; Hayes, M.; Jahnke, F.; Springer, J.; Garcia, A. A., Photon-modulated wettability changes on spiropyran-coated surfaces. *Langmuir* **2002,** *18* (21), 8062-8069.

23. Rosario, R.; Gust, D.; Garcia, A. A.; Hayes, M.; Taraci, J. L.; Clement, T.; Dailey, J. W.; Picraux, S. T., Lotus effect amplifies light-induced contact angle switching. *J. Phys. Chem. B* **2004,** *108* (34), 12640-12642.

24. Fries, K.; Samanta, S.; Orski, S.; Locklin, J., Reversible colorimetric ion sensors based on surface initiated polymerization of photochromic polymers. *Chem Commun* **2008,** (47), 6288-6290.

25. Kessler, D.; Jochum, F. D.; Choi, J.; Char, K.; Theato, P., Reactive Surface Coatings Based on Polysilsesquioxanes: Universal Method toward Light-Responsive Surfaces. *Acs Appl. Mater. Inter.* **2011,** *3* (2), 124-128.

26. Son, S.; Shin, E.; Kim, B.-S., Light-Responsive Micelles of Spiropyran Initiated Hyperbranched Polyglycerol for Smart Drug Delivery. *Biomacromolecules* **2014,** *15* (2), 628-634.

27. Sung, J.; Robb, M. J.; White, S. R.; Moore, J. S.; Sottos, N. R., Interfacial Mechanophore Activation Using Laser-Induced Stress Waves. *J. Am. Chem. Soc.* **2018,** *140* (15), 5000-5003.

28. Blaiszik, B. J.; Baginska, M.; White, S. R.; Sottos, N. R., Autonomic Recovery of Fiber/Matrix Interfacial Bond Strength in a Model Composite. *Advanced Functional Materials* **2010,** *20* (20), 3547-3554.

29. Jones, A. R.; Blaiszik, B. J.; White, S. R.; Sottos, N. R., Full recovery of fiber/matrix interfacial bond strength using a microencapsulated solvent-based healing system. *Compos Sci Technol* **2013,** *79*, 1-7.

30. Zhandarov, S.; Gorbatkina, Y.; Mader, E., Adhesional pressure as a criterion for interfacial failure in fibrous microcomposites and its determination using a microbond test. *Compos Sci Technol* **2006,** *66* (15), 2610-2628.

31. Zhandarov, S.; Mader, E., Indirect estimation of fiber/polymer bond strength and interfacial friction from maximum load values recorded in the microbond and pull-out tests. Part II: Critical energy release rate. *J Adhes Sci Technol* **2003,** *17* (7), 967-980.

32. Zhandarov, S.; Mader, E., Characterization of fiber/matrix interface strength: applicability of different tests, approaches and parameters. *Compos Sci Technol* **2005,** *65* (1), 149-160.

33. Grady, M. E.; Geubelle, P. H.; Braun, P. V.; Sottos, N. R., Molecular Tailoring of Interfacial Failure. *Langmuir* **2014,** *30* (37), 11096-11102.

34. Nygård, P.; Grundke, K.; Mäder, E.; Bellmann, C., Wetting kinetics and adhesion strength between polypropylene melt and glass fibre: influence of chemical reactivity and fibre roughness. *J Adhes Sci Technol* **2002,** *16* (13), 1781-1808.

35. Fujimaki, M.; Kawahara, S.; Matsuzawa, Y.; Kurita, E.; Hayashi, Y.; Ichimura, K., Macrocyclic Amphiphiles. 3. Monolayers of O-Octacarboxymethoxylated Calix[4]resorcinarenes with Azobenzene Residues Exhibiting Efficient Photoisomerizability. *Langmuir* **1998,** *14* (16), 4495-4502.

TOC GRAPHIC

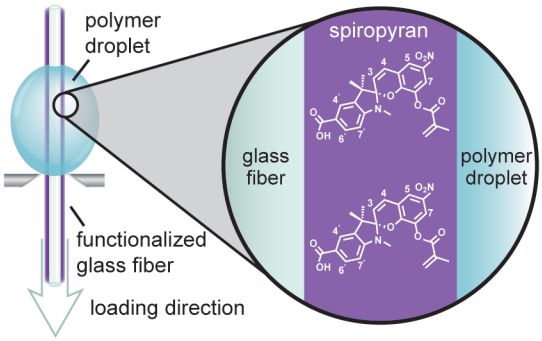
polymer
droplet
functionalized
glass fiber
loading direction
spiropyran
glass
fiber
polymer
droplet